

Use of Raman spectroscopy as an In Situ Tool to Obtain Kinetic Data for Organic Transformations

Jason R. Schmink, Jennifer L. Holcomb, and Nicholas E. Leadbeater*^[a]

Abstract: Raman spectroscopy has been used as an in situ tool to obtain kinetic data for an organic transformation. The model reaction studied was the synthesis of 3-acetylcoumarin from the condensation between salicylaldehyde and ethyl acetoacetate with piperidine as a catalyst. The study shows that precise kinetic data can be obtained quickly and reproducibly, allowing for the facile determination of both

overall reaction order and reaction order with respect to each component of the reaction. Additionally, Arrhenius parameters such as activation energy for a reaction can be readily obtained.

Keywords: activation parameters • kinetics • microwave heating • Raman spectroscopy • reaction mechanisms

In conjunction with computational modeling, this data-rich analysis technique also allows for in-depth probing of mechanistic aspects of reactions. Microwave heating proves to be an ideal tool for aiding in kinetic studies. It offers reproducible noncontact heating as well as precise temperature monitoring and data recording.

Introduction


Microwave heating offers a fast, clean approach to synthesis.^[1] It is often possible to perform reactions in minutes instead of hours and, in many cases, product yields can be improved. Also, as the field progresses, new chemistry is being discovered and developed. An issue with performing a reaction with microwave apparatus is that monitoring its progress generally requires stopping it, allowing the reaction mixture to cool and then using standard analysis techniques such as IR and NMR spectroscopy. As a result, optimization of reaction conditions such as time and temperature is often a matter of trial and error. In the case of inorganic materials chemistry, neutron and X-ray scattering have been used as in situ monitoring tools.^[2,3] These techniques are less applicable to preparative organic chemistry. We have built on the initial work of Pivonka and Empfield^[4] and developed an apparatus for in situ reaction monitoring using Raman spectroscopy.^[5] It has been possible to determine the end-point

of reactions by using this apparatus and we have applied it to a range of synthetic transformations.^[6–8]

While quantitative in situ infrared spectroscopy (e.g., ReactIRTM) has seen significant use for determination of reaction kinetics,^[9,10] there are very few reports of analogous studies with Raman spectroscopy.^[11] In their seminal publication in 2004, Pivonka and Empfield used Raman spectroscopy for the study of a microwave-mediated imine formation reaction and a Knoevenagel condensation.^[4] For the latter reaction, they probed the kinetics of the reaction and also elucidated a reactive intermediate they believed to be formed along the path of the reaction. Having used our in situ Raman apparatus in synthetic chemistry applications, we also wanted to explore the potential for using our experimental set-up for real-time kinetic studies.

In many regards Raman spectroscopy in conjunction with microwave heating is, in principle, an ideal tool for performing kinetic studies. The microwave offers reproducible non-contact heating as well as precise temperature monitoring and data recording. The Raman spectrometer is able to acquire data at such a rate that quantitative data can be extracted for even the most rapid of reactions.^[12] Furthermore, since most spectroscopic techniques require a dark environment for accurate signal measurement, the fact that the microwave cavity is free of significant ambient light is an added advantage. Finally, Raman spectroscopy is in theory an effective means to measure concentration changes in a dynamic system. To probe this and show the potential for

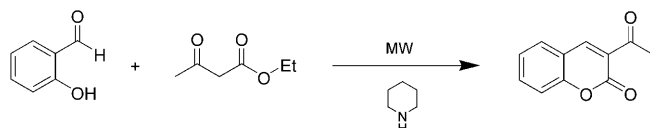
[a] J. R. Schmink, J. L. Holcomb, Dr. N. E. Leadbeater
Department of Chemistry, University of Connecticut
55 North Eagleville Road, Storrs, CT 06269-3060 (USA)
Fax: (+1) 860 617 3518
E-mail: nicholas.leadbeater@uconn.edu

 Supporting information for this article is available on the WWW under <http://dx.doi.org/10.1002/chem.200801158>.

using Raman spectroscopy as a tool for real-time kinetic analysis, we chose as a sharpening stone the synthesis of 3-acetylcoumarin, formed from the base-catalyzed reaction of salicylaldehyde with ethyl acetoacetate. We have previously shown that this reaction can be monitored qualitatively from a synthetic chemistry perspective^[5] and Pivonka and Empfield used an analogous reaction for their kinetic studies^[4] (reaction of salicylaldehyde with benzyl acetoacetate). We wanted to use these foundations to build upon. Our results are presented here. We demonstrate how, using this apparatus, it is possible to quickly and easily obtain valuable kinetic data as well as begin to probe reaction intermediates. We show how we have built on previous work and determined orders of reaction for each reagent in units of concentration as well as Arrhenius parameters for the reaction. In addition, by using our apparatus in conjunction with calculations, we propose a mechanistic pathway for the reaction that differs from that originally proposed.

Results and Discussion

Coumarins have been found to have multibiological activities.^[13] They can be prepared by using a number of synthetic routes^[14] and microwave heating has been used as a tool.^[15] In our model reaction shown in Scheme 1 (synthesis of 3-



Scheme 1. Reaction of salicylaldehyde with ethyl acetoacetate to yield 3-acetylcoumarin.

acetylcoumarin from salicylaldehyde with ethyl acetoacetate), we used piperidine as the catalyst and ethyl acetate as the solvent. While this reaction on the outset looks simple, the precise mechanism is still a matter of debate and small changes in the system may result in very different reaction pathways.^[16] This added to our motivation to probe the reaction in detail. Upon inspection of the Raman spectra of salicylaldehyde, ethyl acetoacetate, and 3-acetylcoumarin we found that there are two clearly defined signals in the product (1563 cm^{-1} , 1608 cm^{-1}) that are not present in the starting materials, so it is one of these (1608 cm^{-1}) that we decided to follow in our reaction. The spectrum of 3-acetylcoumarin taken in ethyl acetate with signals due to solvent subtracted is shown in Figure 1.

To determine the nature of the stretching mode observed at 1608 cm^{-1} we used a computational approach. The stretching modes for 3-acetylcoumarin were calculated using Gaussian 03,^[17] applying the Becke exchange functional^[18] (B) coupled with the correlation functional developed by Lee, Yang, and Parr^[19] (LYP) at the 6-31G(d) basis set. The calculations yielded an intense signal at 1666 cm^{-1} which,

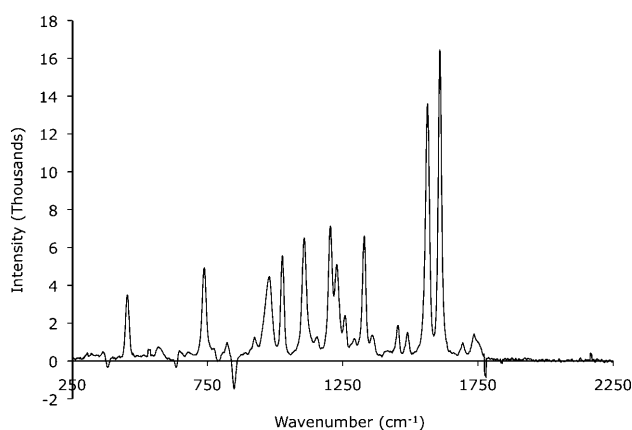


Figure 1. Raman spectrum of 3-acetylcoumarin (0.35 M in ethyl acetate) with signals due to solvent subtracted

after application of the appropriate scaling factor,^[20] correlated to a stretching frequency of 1602 cm^{-1} , fitting well with our observed value of 1608 cm^{-1} . The complex stretching mode is shown in Figure 2.

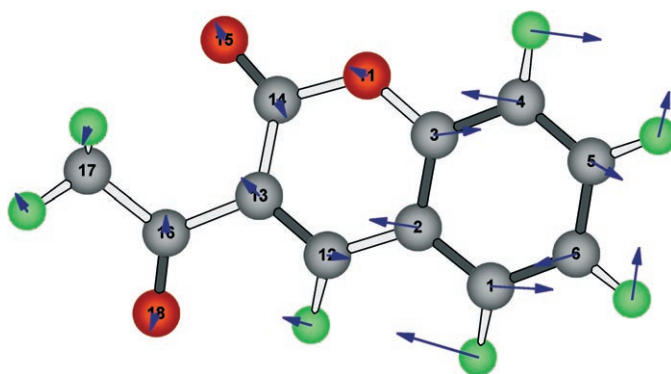


Figure 2. Stretching mode giving rise to the observed Raman peak at 1602 cm^{-1} as calculated at the B3LYP-6/31G(d) theory level (observed 1608 cm^{-1})

Experimental considerations: The majority of microwave-promoted reactions are performed using sealed tubes. To ensure precise reaction monitoring conditions, for our kinetic studies here we opted for an open-vessel configuration. First, the salicylaldehyde, ethyl acetoacetate, and the ethyl acetate solvent were brought to reflux at which point a background scan was taken. Having the reaction at the desired temperature before the catalyst was added alleviated any peak intensity variation due to temperature effects during a specific experiment. Second, this set-up allowed for a quantitative $t=0$ spectrum to be obtained. The formation of the coumarin can be effected at room temperature, so addition of piperidine to the reaction mixture prior to heating (e.g., under sealed-vessel conditions) would initiate the reaction before the introduction into the microwave cavity. Finally, to determine kinetic parameters accurately, it was es-

essential to have the reaction at the desired reaction temperature before adding the catalyst. Adding piperidine prior to heating leads to dynamic, and consequently imprecise, kinetic data being obtained during the ramp to the desired temperature. While these issues are not crucial when monitoring reactions in a qualitative manner, our desire to develop the Raman spectrometer/microwave interface as a quantitative tool demanded this precise control of reaction parameters.

Obtaining a calibration curve: To be able to measure product concentration accurately and ultimately derive rate laws, a calibration curve was required to translate signal strength of the peak forming at 1608 cm^{-1} into units of concentration in standard terms. To achieve this, solutions of known concentrations of 3-acetylcoumarin in ethyl acetate were prepared. They were sequentially placed inside a round-bottomed flask inside the microwave cavity, brought to reflux ($83\text{--}84^\circ\text{C}$) using microwave irradiation and the Raman spectrum collected. After subtraction of signals due to the solvent, a plot of signal intensity at 1608 cm^{-1} versus concentration was made (Figure 3) which yielded a straight line ($R^2 = 0.9986$).

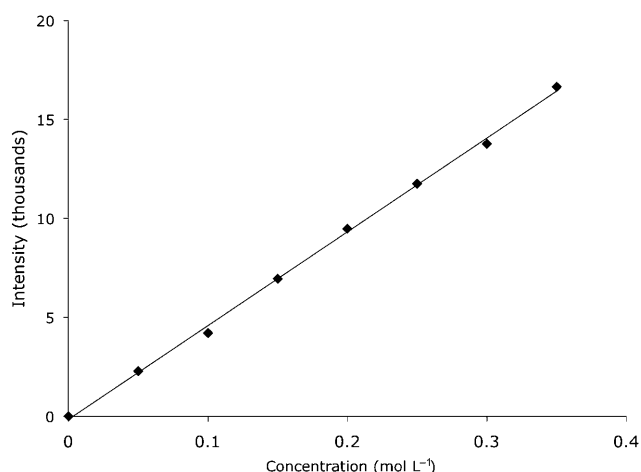


Figure 3. Plot of Raman signal intensity of the peak arising at 1608 cm^{-1} versus [3-acetylcoumarin] yielding a line, $f(x) = mx + b$; $x = [3\text{-acetylcoumarin}]$ in mol L^{-1} , $m = 47.393$; $R^2 = 0.9986$

Temperature scaling factor: When monitoring reactions using Raman spectroscopy at different temperatures it is important to take into account that fact that the Stokes Raman band (which is being monitored) is inversely proportional to temperature. This relationship is due to the fundamental manner in which Raman spectroscopy probes a molecule; that is it excites it in the lowest energy electronic state. As temperature increases, there is a smaller population of molecules in that ground state to be excited, and so the signal intensity drops. This being said, over small temperature ranges the change in the Stokes shift is fairly negligible, but, for analytical accuracy, we deemed it important in our study to determine an appropriate scaling factor that would allow us to compare peak intensities at different tem-

peratures with confidence.^[21] This was achieved by measuring the intensity of the 1608 cm^{-1} signal of known concentrations of 3-acetylcoumarin at temperatures within our range of interest. The average of ten scans at five temperatures ranging from $35\text{--}75^\circ\text{C}$ and at four different concentrations gave a total of 20 data points (Figure 4). From this, a scaling factor was determined.

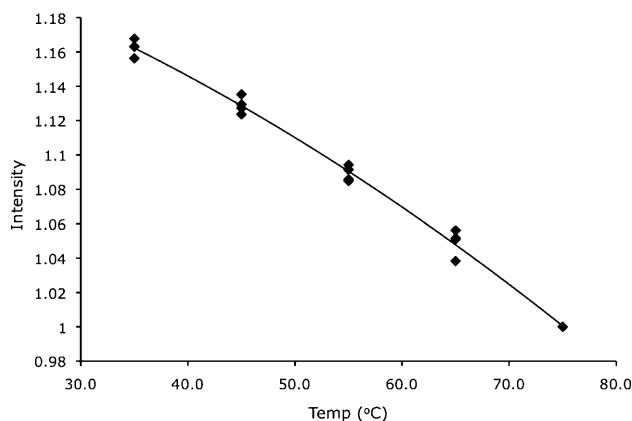


Figure 4. Plot of Raman signal intensity vs. temperature at constant concentrations. A second-order polynomial proved the best fit line over the temperature range: $f(T) = (-2.259 \times 10^{-5} T^2 - 1.558 \times 10^{-3} T + 1.244)^{-1}$; T in $^\circ\text{C}$, $R^2 = 0.9934$

Determination of reaction orders: With the appropriate calibration curve and scaling factor in hand, we wanted to use the apparatus to determine the order of the reaction with respect to each reagent. We postulated that precise reaction rates could be determined by running a series of experiments by varying concentrations of reagents and monitoring the appearance of the signal at 1608 cm^{-1} due to product formation followed by conversion of units of Raman intensity to units of molarity. To achieve this we set up a series of reactions based around the kinetic method of initial rates (varying the concentration of one reagent at a time and measuring the rate of reaction at $t = 0$) in conjunction with the isolation method (performing experiments in which the concentration of one or more reagents is kept constant to determine rate dependence as a function of the reagent being probed). We decided to focus attention initially on the order of the reaction with respect to the piperidine catalyst. Holding the concentrations of salicylaldehyde and ethyl acetoacetate constant at 1.00 M , an initial range of piperidine concentrations were screened, ranging from 0.0200 M to 0.400 M , the data being shown in Figure 5. At low catalyst loadings ($0.0200\text{--}0.0800\text{ M}$) the reaction appears to be first-order with respect to the piperidine concentration. However, at increasing catalyst loading, it becomes apparent that the piperidine is implicated in numerous reversible steps in the reaction mechanism and is of a complex order, since there is significant deviation from linearity. At these higher catalyst concentrations, the reaction rate is approximately proportional to the square root of the concentration of pi-

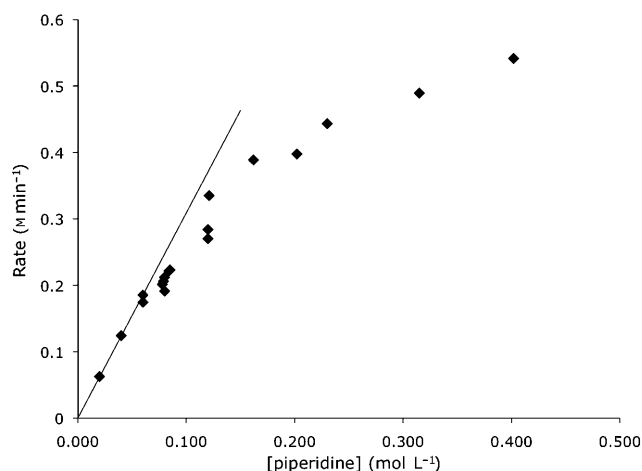


Figure 5. Plot of rate of formation of 3-acetylcoumarin as monitored by the peak forming at 1608 cm^{-1} versus piperidine concentration. Increasing concentrations above 0.0800 M show loss of linear dependence on catalyst loading. Note: a linear approximation can be made at low catalyst loadings.

piperidine used. The general rate law is given in Equation (1) in which $f([\text{piperidine}]) \approx [\text{piperidine}]^1$ for concentrations below 0.080 M , and $f([\text{piperidine}]) \approx [\text{piperidine}]^{1/2}$ for concentrations from 0.100 – 0.400 M

$$\text{rate} = k [\text{salicylaldehyde}]^a [\text{ethyl acetoacetate}]^b f([\text{piperidine}]) \quad (1)$$

The complex nature of the rate dependence upon the catalyst concentration is not totally unexpected. The piperidine could be imagined to be involved in a range of equilibrium processes. The $\text{p}K_a$ values in dimethyl sulfoxide (DMSO) for the piperidinium cation, the phenolic proton of the salicylaldehyde, and the acidic proton of ethyl acetoacetate are 10.9 , 14.8 , and 14.1 , respectively.^[22]

We next turned attention to determining the order of the reaction with respect to ethyl acetoacetate and salicylaldehyde. We decided to perform the kinetic measurements at a piperidine concentration of 0.0800 M . To simplify our future calculations we reformulated Equation (1) to give us Equation (2), in which rate_{obs} and k_{obs} are the rate and rate constant at 0.0800 M piperidine catalyst loading.

$$\text{rate}_{\text{obs}} = k_{\text{obs}} [\text{salicylaldehyde}]^a [\text{ethyl acetoacetate}]^b \quad (2)$$

All subsequent calculations could then be performed in terms of rate_{obs} and k_{obs} . In the first series of experiments, initial rates were measured as a function of various concentrations of ethyl acetoacetate (0.0312 – 2.00 M) holding the salicylaldehyde concentration constant at 1.00 M and the piperidine concentration constant at 0.0800 M . Again the appearance of the signal at 1608 cm^{-1} due to product formation was monitored and the units of Raman intensity were converted to molarity values. At ethyl acetoacetate concentra-

tions of 0.125 , 0.250 , and 0.500 M , the reaction rate was linear for approximately the first 60 s or six scans before beginning to deviate from linearity. Data obtained in the linear region is gathered in Table 1 and shown graphically in

Table 1. Data for the signal growing in at 1608 cm^{-1} [intensity s^{-1}] and conversion to units of rate [M min^{-1}] in the linear region at various concentrations of salicylaldehyde.

[aldehyde]	[intensity s^{-1}]	rate _{obs} [M min^{-1}]
2.00	314	0.398
1.00	167	0.211
0.50	81.7	0.103
0.25	44.4	0.056
0.125	24.3	0.031
0.063	17.1	0.022
0.031	9.41	0.012

Figure 6. At concentrations of 0.0625 M and lower, the detection limit of the Raman spectrometer set to 10 s integrations became a factor. At concentrations of 1.00 M linearity is

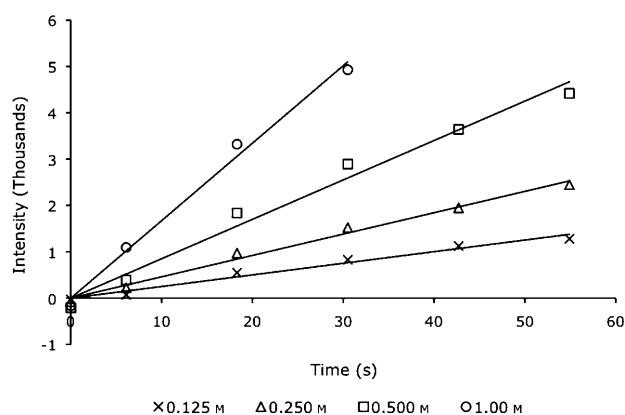


Figure 6. Plot of Raman signal intensity due to the peak growing in at 1608 cm^{-1} versus time in the linear region at various concentrations of salicylaldehyde, holding [ethyl acetoacetate] at 1.0 M .

maintained for only approximately the first 30 s (4 data points) of the reaction. At the 2.00 M concentration, the signal intensity's deviation from linearity was so rapid that at most three points could be used to determine the initial rate. As such, this data was deemed unusable. The experiments were then repeated, holding the initial concentration of ethyl acetoacetate at a constant 1.00 M and similarly varying the concentrations of salicylaldehyde (Figure 7; Table 2). For both ethyl acetoacetate and salicylaldehyde, a plot of rate of reaction versus initial concentration gives a straight line showing that the reaction is first order in both of these reagents. Thus the overall rate equation is given by Equation (3) in which rate_{obs} and k_{obs} are the rate and rate constant at 0.08 M piperidine catalyst loading or, more fully, by Equation (4) in which $f([\text{piperidine}]) \approx [\text{piperidine}]^1$ for concentrations below 0.080 M , and $f([\text{piperidine}]) \approx [\text{piperidine}]^{1/2}$ for concentrations from 0.100 – 0.400 M

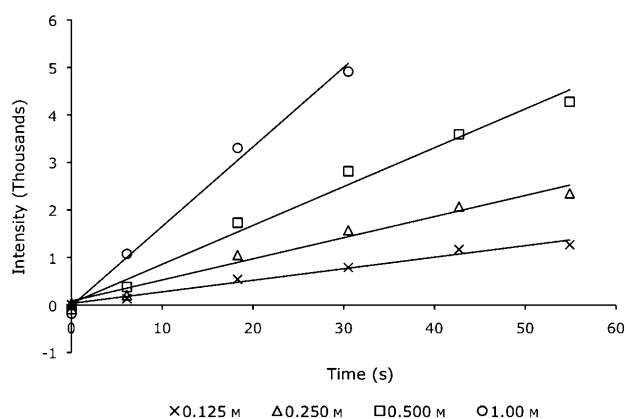


Figure 7. Plot of Raman signal intensity due to the peak growing in at 1608 cm^{-1} versus time in the linear region at various concentrations of ethyl acetoacetate, holding [salicylaldehyde] at 1.0 M .

Table 2. Data for the signal growing in at 1608 cm^{-1} [intensity s^{-1}] and conversion to units of rate [M min^{-1}] in the linear region at various concentrations of ethyl acetoacetate.

[ethyl acetoacetate]	[intensity s^{-1}]	rate _{obs} [M min^{-1}]
2.00	304	0.385
1.00	167	0.211
0.50	85.1	0.108
0.25	46.1	0.058
0.125	25.1	0.032
0.063	15.2	0.019
0.031	10.8	0.014

$$\text{rate}_{\text{obs}} = k_{\text{obs}} [\text{salicylaldehyde}]^1 [\text{ethyl acetoacetate}]^1 \quad (3)$$

$$\text{rate} = k [\text{salicylaldehyde}]^1 [\text{ethyl acetoacetate}]^1 f([\text{piperidine}]) \quad (4)$$

Determination of activation energy: Having obtained kinetic data to ascertain the orders of the reagents our next objective was to determine the activation energy (E_a) for the reaction. This was achieved by running the reaction at a range of temperatures between 25 and 80°C . The reactions were performed using 1 M concentrations of ethyl acetoacetate and salicylaldehyde and 0.08 M piperidine and the product signal at 1608 cm^{-1} was monitored. After translating Raman signal intensity to units of concentration using our calibration curve and then compensating for temperature effects using our temperature scaling factor, we obtained rate constant data (k_{obs}) in units of $\text{M}^{-1}\text{min}^{-1}$ (Table 3). Plotting $\ln k_{\text{obs}}$ versus $1/T$ (Figure 8) gave a straight line, the slope of which corresponds to $-E_a/R$, ($R = 8.314\text{ J K}^{-1}\text{mol}^{-1}$). From this, the activation energy for the reaction was calculated to be 38.3 kJ mol^{-1} .

The quantitative data obtained was then used to extrapolate and calculate a rate constant (k_{obs}) for other reaction temperatures. We wanted to compare our results here with

Table 3. Data for the signal growing in at 1608 cm^{-1} for 3-acetylcoumarin in units of Raman intensity s^{-1} , subsequent temperature-corrected (T_c) values by using Equation (5), and conversion to units of k_{obs} [$\text{M}^{-1}\text{s}^{-1}$] at various temperatures.

T [K]	$1/T$	slope [IU s^{-1}]	scaled slope T_c [IU s^{-1}]	k_{obs} [$\text{M}^{-1}\text{min}^{-1}$]	\pm	$\ln k_{\text{obs}}$
309.65	0.003229	27.8	24	0.0304	0.0018	-3.4945
320.3	0.003122	45.8	40.8	0.0517	0.0063	-2.9620
330.25	0.003028	68.4	63.2	0.0801	0.0009	-2.5248
340.8	0.002934	100.2	96.7	0.1224	0.0048	-2.1002
350.15	0.002856	132	133.5	0.1690	0.0050	-1.7779

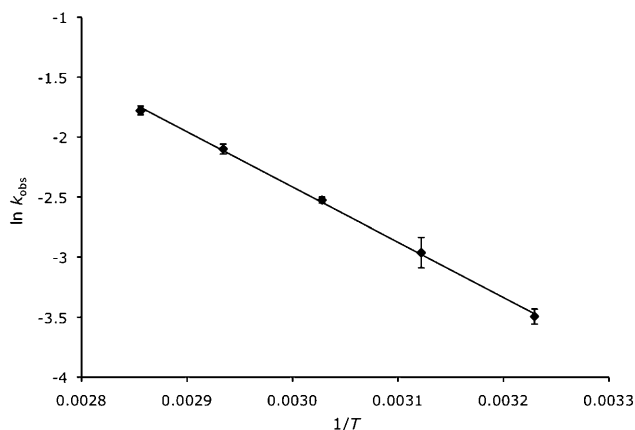
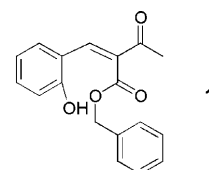


Figure 8. Plot of $\ln k_{\text{obs}}$ versus $1/T$ yielding a straight line, $y = mx + b$, $m = E_a/R = 4602$, $b = 11.407$, $R^2 = 0.9990$, average of 2 trials at each temperature.

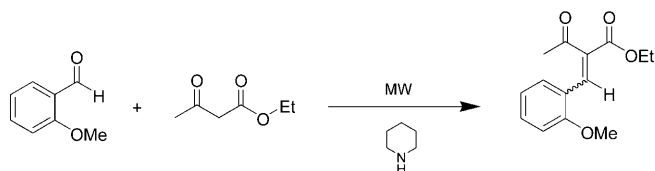
those we obtained for our qualitative studies previously when using the Raman apparatus simply as a tool for monitoring how long the reaction took to reach completion.

Performing the reaction at 130°C we found that it took approximately 8 min to reach completion. Extrapolating our quantitative rate data to 130°C we found that $k_{\text{obs}} = 0.972\text{ M}^{-1}\text{min}^{-1}$ or $0.0162\text{ M}^{-1}\text{s}^{-1}$. Using the half-life equation for a second-order reaction ($t_{1/2} = 1/k_{\text{obs}}$), we calculated the half-life for the reaction at 130°C to be 62 seconds. After six half-lives ($\approx 6\text{ min}$) the projected yield would be $\approx 98.4\%$; this corresponded with the observed product yields in the reaction and fits well with our previous qualitative results.

Mechanistic insight: Our next objective was to probe the mechanism of the reaction knowing the first-order dependence on both the concentrations of ethyl acetoacetate and salicylaldehyde. In their study Pivonka and Empfield saw evidence for the formation of a transient intermediate in the reaction of salicylaldehyde and benzyl acetoacetate.^[4] They proposed that the intermediate, **1**, was the result of a Knoevenagel condensation. This seemed surprising to us given that the restricted rotation about the $\text{C}=\text{C}$ double bond would limit product formation to a 50% theoretical yield, but



obtained product yields for the reaction are high, generally greater than 90%. The two key reactions taking place in their reaction and also ours are the Knoevenagel condensation and a transesterification. We decided to perform series of experiments using model substrates with the aim of determining in which order these reactions occur. To address the Knoevenagel condensation component we used *o*-anisaldehyde as a test substrate (Scheme 2). With this, while a Kno-



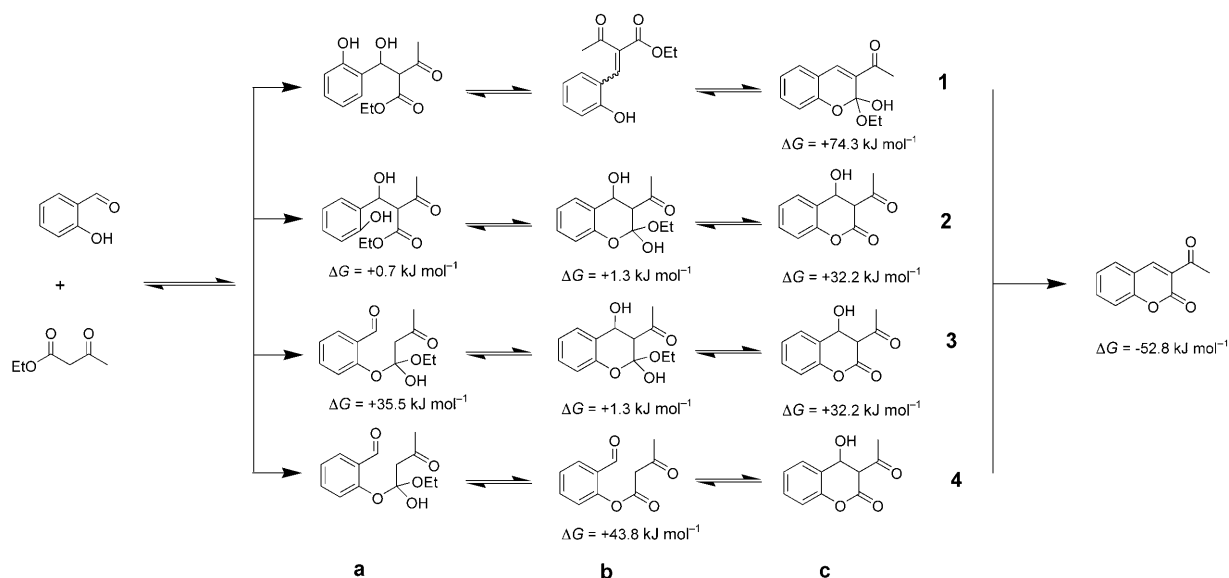
Scheme 2. Reaction of *o*-anisaldehyde with ethyl acetoacetate to yield ethyl-(*E/Z*)-2-acetyl-3-(2-methoxyphenyl)-acrylate.

venagel condensation with ethyl acetoacetate can take place, there is no potential for cyclization. We performed a range of kinetic measurements holding the reagents at 1.00 M in ethyl acetate, and again using 0.08 M piperidine as the catalyst and monitored formation of the carbon–carbon double bond (Raman signal at 1601 cm⁻¹). From the outset it was clear that the reaction with *o*-anisaldehyde was much slower than that using salicylaldehyde and that no observable reaction took place below 35 °C within 10 min of monitoring. Plotting the observed rate constants we obtained at higher temperatures versus 1/*T* gave a straight line, from which the activation energy for the reaction was calculated to be 51.3 kJ mol⁻¹, significantly higher than for the condensation to form 3-acetylcoumarin (38.3 kJ mol⁻¹). The fact that the activation energy is higher when using *o*-anisaldehyde is not too surprising. The product shows significant de-

viation from planarity and the energy taken for the condensation step and concomitant formation of the carbon–carbon double bond could be imagined to be quite high. Analysis of a product mixture from the reaction with *o*-anisaldehyde showed the expected *E* and *Z* isomers of the condensation product.

There are four plausible mechanistic pathways that would exhibit first-order dependence upon both salicylaldehyde as well as ethyl acetoacetate, denoted as 1, 2, 3 and 4 in Scheme 3. Path 1 is the complete Knoevenagel-type reaction followed by ring closure proposed by Pivonka and Empfield. We know that the activation energy for our model substrate *o*-anisaldehyde was significantly higher than that observed in the reaction with salicylaldehyde. Moreover, the relative energy for intermediate **1c** was calculated to 74.3 kJ mol⁻¹, much higher than the observed activation energy for the reaction. Based on these results, as well as the issues of restricted rotation about the C=C double bond, we believe that this is not the mechanism for the reaction. Path 4 involves full transesterification followed by lactone formation with loss of ethanol and then dehydration to form the product. Calculation of the relative energy of intermediate **4b** along this pathway shows that the formation of the initial transesterified compound requires more energy than the calculated activation energy thereby ruling out this pathway. Path 2 involves partial Knoevenagel reaction followed by cyclization, concomitant loss of ethanol, and finally dehydration to yield the product. Path 3 involves partial transesterification reaction followed by cyclization, carbon–carbon bond formation, loss of ethanol, and then dehydration to yield the product. One of these two mechanisms seems the most likely and fit our recorded kinetic data.

Observation of transient intermediates: In an attempt to probe the mechanism further, we plotted in three dimen-



Scheme 3. The 4 most plausible reaction pathways for formation 3-acetylcoumarin from salicylaldehyde and ethyl acetoacetate.

sions the formation of the 3-acetylcoumarin product as a function of time and Raman intensity. Careful analysis of the 3D profile in the region between 1500–1680 cm^{-1} shows evidence for the formation and subsequent consumption of a transient intermediate (Figure 9). A peak with a local

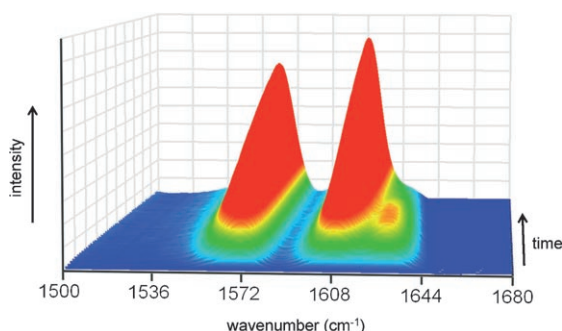


Figure 9. Formation of 3-acetylcoumarin as a function of time and Raman intensity in the region from 1500 to 1680 cm^{-1} during the first 10 min of the reaction.

maximum at 1630 cm^{-1} grows in rapidly and then disappears over the course of the reaction. This is clearly seen when normalized Raman signal intensities for the intermediate and the product are plotted versus time (Figure 10). We believe that the intermediate formed is most likely **2b/3b**. The optimized structure is calculated to have a very low energy ($\Delta G = +1.3 \text{ kJ mol}^{-1}$ vs. starting materials) and a calculated Raman frequency slightly higher than the acetylcoumarin product (1605 vs. 1602 cm^{-1}). Though computational modeling predicts a slightly higher Raman active vibrational frequency for intermediate **2c/3c** as well, the relative energy calculated is such that we believe there would not be a sufficient population to be observable by Raman spectroscopy under these conditions. No other intermediates modeled are calculated to have a Raman active frequency between 1600 and 1650 cm^{-1} . Moreover, the addition of piperidine catalyst to a 1.00 M solution of salicylaldehyde in ethyl acetate gives

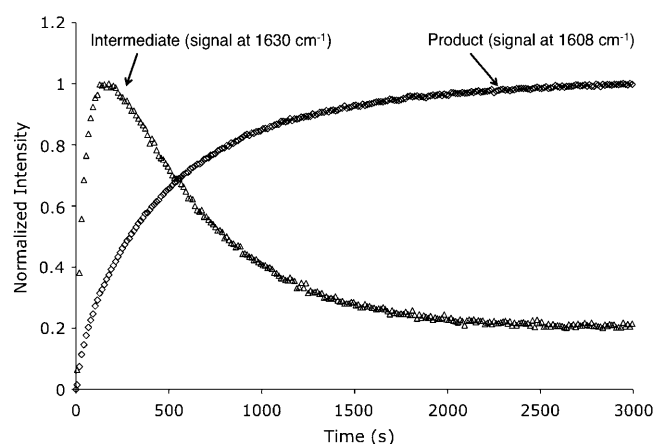


Figure 10. Plot of normalized signal intensity versus time for the Raman signals at 1630 and 1608 cm^{-1} .

rise to no new peaks in this region. The same can be said for the addition of piperidine to a solution of ethyl acetoacetate; no new peaks arise within the Raman spectrum. Therefore, the observable intermediate must be a new adduct between the salicylaldehyde and ethyl acetoacetate with a low enough energy so as to build a sufficient population as to be observable by Raman spectroscopy under these conditions, thus implicating intermediate **2b/3b**. However, even with a putative characterization of the intermediate formed during the reaction, it is still not possible to differentiate between mechanisms 2 and 3.

Conclusion

We have built on previous work showing that Raman spectroscopy can be employed as an in situ tool to obtain kinetic data for organic transformations. The model reaction studied shows that precise kinetic data can be obtained quickly and reproducibly, allowing for the facile determination of both overall reaction order and reaction order with respect to each component of the reaction. Additionally, Arrhenius parameters such as activation energy for a reaction can be readily obtained. This data-rich analysis technique also allows for in-depth probing of mechanistic aspects of reactions, especially when used in conjunction with results from computational chemistry. Furthermore, microwave heating proves to be an ideal tool for aiding in kinetic studies, offering reproducible noncontact heating as well as precise temperature monitoring and data recording. Investigations are currently underway to exploit further the full potential of this combination of microwave heating and in situ Raman spectroscopy with regard to kinetic studies of other reactions.

Experimental Section

General experimental: All reagents were obtained from commercial suppliers (Sigma-Aldrich or Fisher) and used without further purification. ^1H and ^{13}C NMR spectra were recorded at 293 K on a 300 MHz spectrometer.

Apparatus: Reactions were conducted using a monomode microwave unit (CEM Discover® S-Class) interfaced with a Raman spectrometer (Enwave Optronics) and is described in detail elsewhere and in the Supporting Information.

Typical procedure for monitoring the formation of 3-acetylcoumarin: Salicylaldehyde (6.106 g, 50.00 mmol) and ethyl acetoacetate (6.507 g, 50.00 mmol) were placed in a 50.00 mL volumetric flask. The reagents were diluted with ethyl acetate (final volume 50.00 mL). This solution was transferred to a 50 mL long-necked round-bottomed flask equipped with a Teflon-coated stirbar. The flask was placed into the microwave cavity, making sure that any company glassware markings were orthogonal to the Raman laser path. The microwave attenuator was then locked in place. A 5 cm adapter was connected to the round-bottomed flask to allow a Claisen adapter with septum inlet to be placed atop the reaction flask. A reflux condenser was placed on the Claisen adapter. The septum inlet was capped with a rubber stopper with a 22-gauge syringe needle inserted through. The Raman probe was inserted into the microwave cavity until the quartz light pipe just made contact with the side of the reaction

flask. The reaction mixture was brought to reflux (83–84°C), at which point a background scan of the reaction that would be subtracted from all subsequent scans was taken. The Raman spectrometer was set to take a scan every 10 s. and continuous scans commenced. After the first scan ($t=0$), the piperidine catalyst (436 mg, 4.0 mmol, 8 mol%) was rapidly injected into the reaction mixture through the septum in the Claisen adaptor. After running the reaction for the requisite period of time, the Raman data acquisition and the microwave heating were halted. The reaction mixture was allowed to cool to room temperature and the product isolated was stopped. Upon cooling, the product was collected by vacuum filtration and recrystallized from ethanol. ^1H NMR (300 MHz, CDCl_3): $\delta=8.51$ (s, 1H), 7.67 (m, 2H), 7.40 (m, 2H), 2.73 ppm (s, 3H). ^{13}C NMR (300 MHz, CDCl_3): $\delta=195.4$, 159.2, 155.3, 147.4, 134.4, 130.2, 125.0, 124.5, 118.2, 116.7, 30.5 ppm.

Acknowledgement

The University of Connecticut Research Foundation is thanked for funding and Enwave Optronics and CEM Corp for equipment support. The authors acknowledge Robert Bohn for advice and Robert Birge for allowing use of the Anamol software package.

- [1] A number of books on microwave-promoted synthesis have been published; see for example: *Microwaves in Organic Synthesis* (Ed.: A. Loupy), Wiley-VCH, Weinheim, 2006.
- [2] For a review see: G. A. Tompsett, W. C. Conner, K. S. Yngvesson, *ChemPhysChem* **2006**, 7, 296.
- [3] G. R. Robb, A. Harrison, A. G. Whittaker, *PhysChemComm* **2002**, 135.
- [4] D. E. Pivonka, J. R. Empfield, *Appl. Spectrosc.* **2004**, 58, 41.
- [5] For an overview of the equipment, see: N. E. Leadbeater, J. R. Schmink, *Nat. Protoc.* **2008**, 3, 1.
- [6] N. E. Leadbeater, R. J. Smith, *Org. Lett.* **2006**, 8, 4588.
- [7] N. E. Leadbeater, R. J. Smith, T. M. Barnard, *Org. Biomol. Chem.* **2007**, 5, 822.
- [8] N. E. Leadbeater, R. J. Smith, *Org. Biomol. Chem.* **2007**, 5, 2770.
- [9] For selected recent examples in organic chemistry see: a) I. Poljansek, B. Likozar, M. Krajnc, *J. Appl. Polym. Sci.* **2007**, 106, 878; b) S. E. Denmark, S. M. Pham, R. A. Stavenger, X. P. Su, K. T. Wong, Y. Nishigaichi, *J. Org. Chem.* **2006**, 71, 3904; c) M. Grabarnick, S. Zamir, *Org. Process Res. Dev.* **2003**, 7, 237; d) A. Pintar, J. Batista, J. Levec, *Analyst* **2002**, 127, 1535.
- [10] For selected recent examples in catalysis see: a) A. R. Almeida, J. A. Moulijn, G. Mul, *J. Phys. Chem. C* **2008**, 112, 1552; b) G. Koster, J. U. Huh, R. H. Hammond, M. R. Beasley, *Appl. Phys. Lett.* **2007**, 90, 261917; c) D. Tibiletti, F. C. Meunier, A. Goguet, D. Reid, R. Burch, M. Boaro, M. Vicario, A. Trovarelli, *J. Catal.* **2006**, 244, 183; d) G. A. H. Mekhemer, S. A. Halawy, M. A. Mohamed, M. I. Zaki, *J. Catal.* **2005**, 230, 109.
- [11] a) D. D. Waal, A. M. Heynes, *J. Solid State Chem.* **1989**, 80, 170; b) M. E. Ehly, P. J. Gemperline, A. Nordon, D. Littlejohn, J. K. Basford, M. De Cecco, *Anal. Chim. Acta* **2007**, 595, 80.
- [12] For a recent kinetic study not involving in situ spectroscopy see: J. P. Gilday, P. Lenden, J. D. Moseley, B. G. Cox *J. Org. Chem.* **2008**, 73, 3130.
- [13] For a recent review see: M. V. Kulkarni, G. M. Kulkarni, C. H. Lin, C. M. Sun, *Curr. Med. Chem.* **2006**, 13, 2795.
- [14] For an overview see: J. D. Hepworth, C. D. Gabbut, B. M. Heron in *Comprehensive Heterocyclic Chemistry II Vol. 5* (Eds.: A. R. Katritzky, C. W. Rees, E. F. V. Scriven, A. McKillop), Pergamon, Oxford, **1996**, Chapter 8.
- [15] a) L. C. Rong, X. Y. Li, D. Q. Shi, S. J. Tu, Q. Y. Zhuang, *Synth. Commun.* **2007**, 37, 183; b) B. Rajitha, V. N. Kumar, P. Someshwar, J. V. Madhav, P. N. Reddy, Y. T. Reddy, *ARKIVOC* **2006**, 23; c) K. M. Al-Zaydi, *Molecules* **2003**, 8, 541; d) S. Frere, V. Thiery, T. Besson, *Tetrahedron Lett.* **2001**, 42, 2791; e) A. de la Hoz, A. Moreno, E. Vazquez, *Synlett* **1999**, 608; f) D. Bogdal, *J. Chem. Res. Miniprint* **1998**, 468.
- [16] For a historical perspective of the Knoevenagel reaction see: G. Jones, *Org. React.* **1967**, 15, 204.
- [17] Gaussian 03, Revision B.01, M. J. Frisch, G. W. Trucks, H. B. Schlegel, G. E. Scuseria, M. A. Robb, J. R. Cheeseman, J. A. Montgomery, Jr., T. Vreven, K. N. Kudin, J. C. Burant, J. M. Millam, S. S. Iyengar, J. Tomasi, V. Barone, B. Mennucci, M. Cossi, G. Scalmani, N. Rega, G. A. Petersson, H. Nakatsuji, M. Hada, M. Ehara, K. Toyota, R. Fukuda, J. Hasegawa, M. Ishida, T. Nakajima, Y. Honda, O. Kitao, H. Nakai, M. Klene, X. Li, J. E. Knox, H. P. Hratchian, J. B. Cross, V. Bakken, C. Adamo, J. Jaramillo, R. Gomperts, R. E. Stratmann, O. Yazyev, A. J. Austin, R. Cammi, C. Pomelli, J. W. Ochterski, P. Y. Ayala, K. Morokuma, G. A. Voth, P. Salvador, J. J. Dannenberg, V. G. Zakrzewski, S. Dapprich, A. D. Daniels, M. C. Strain, O. Farkas, D. K. Malick, A. D. Rabuck, K. Raghavachari, J. B. Foresman, J. V. Ortiz, Q. Cui, A. G. Baboul, S. Clifford, J. Cioslowski, B. B. Stefanov, G. Liu, A. Liashenko, P. Piskorz, I. Komaromi, R. L. Martin, D. J. Fox, T. Keith, M. A. Al-Laham, C. Y. Peng, A. Nanayakkara, M. Challacombe, P. M. W. Gill, B. Johnson, W. Chen, M. W. Wong, C. Gonzalez, J. A. Pople, Gaussian, Inc., Wallingford, CT, **2004**.
- [18] A. D. Becke, *Phys. Rev. A* **1988**, 38, 3098.
- [19] C. Lee, W. Yang, R. G. Parr, *Phys. Rev. B* **1988**, 37, 785.
- [20] A. P. Scott, L. Radom, *J. Phys. Chem.* **1996**, 100, 16502.
- [21] For previous examples of the derivation of temperature scaling factors in Raman spectroscopy see: a) A. L. Chakraborty, R. K. Sharma, M. K. Saxena, S. Kher, *Opt. Commun.* **2007**, 274, 396; b) T. R. Hart, R. L. Aggarwal, B. Lax, *Phys. Rev. B* **1970**, 1, 638.
- [22] <http://www.chem.wisc.edu/areas/reich/pkatable/index.html>

Received: June 12, 2008
Published online: October 1, 2008